JOURNAL OF SOLID STATE CHEMISTRY 53, 290–302 (1984)

Microscopic Mechanism of Decomposition of Fe-Doped β''-Alumina

N. OTSUKA, H. SATO, T. Y. TSENG, AND R. W. VEST

School of Materials Engineering, Purdue University, West Lafayette, Indiana 47907

Received September 27, 1983; in revised form February 8, 1984

The role of conduction layers in a decomposition process of Fe-doped β''-alumina into Na-ferrite and spinel in a reducing atmosphere was investigated by means of high resolution transmission electron microscopy. The decomposition starts as diffusion of Na ions out from conduction layers of decomposing β''-alumina into surrounding β''-alumina, causing the collapsing of conduction layers. This leads to a removal of some oxygen ions which is accompanied by a change of Fe^{3+} ions to Fe^{2+} ions. The reaction further proceeds as the formation of precipitates of Na-ferrites and as the reconstruction around the conduction layers, resulting in the formation of spinel. A reverse reaction of the decomposed phases into β''-alumina occurs by annealing in air. Individual conduction layers are recreated in spinel by the flow of ions from the remaining β''-alumina and precipitated Na-ferrite, leading to the recovery into β''- alumina, along with a reverse change of Fe^{2+} to Fe^{3+}.

Introduction

β-alumina type compounds, β-alumina, and β''-alumina and their derivatives, are among the most promising solid electrolytes at this time (*1–3*). Their structures are described as periodic modulations of spinel by loose (conduction) layers (*4, 5*). Therefore, β- and β''-alumina are structurally very similar and differ only in the stacking symmetry of close-packed oxygen layers. The existence of the loose layers is responsible for the high ionic conductivity of these compounds. These compounds, especially β''-alumina, are, however, susceptible to degradation, and the sensitivity to the degradation has been attributed also to the unique structure of these compounds.

The application of Fe-doped β- and β''-alumina as electrodes to be used with β-alumina type compounds as electrolytes has been investigated by Vest and his collaborators (*6–8*). During this study Fe-doped β''-alumina utilized as an electrode was found to decompose at a hot-pressing stage onto Li β-alumina solid electrolyte at 1150°C in N_2 atmosphere, but to recover by a following annealing at 600°C in air (*8*). Therefore, we investigated the mechanism of this reversible process by means of high resolution transmission electron microscopy with an intention to confirm the role of conduction layers in solid state reactions of this type of compound in general.

In the following, general features of the decomposition and the recovery processes are first described as investigated by means of X-ray powder pattern technique. Then the decomposition products at different stages of reaction investigated by high resolution TEM are presented. We then organize and piece together these observations

0022-4596/84 $3.00

Copyright © 1984 by Academic Press, Inc.
All rights of reproduction in any form reserved.

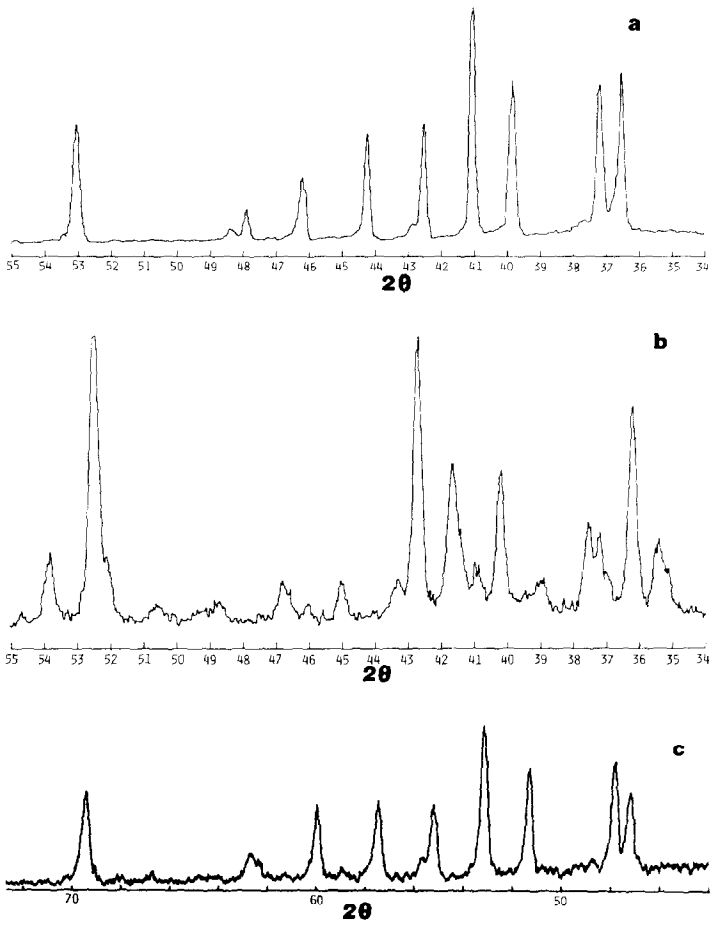

FIG. 1. X-Ray powder patterns of the original (a), decomposed (b), and (c) recovered specimens. The recovered specimen used for (c) here was annealed at 1400°C for 1 hr in air to show a complete recovery. Cr$K\alpha$ radiation instead of Co$K\alpha$ radiation was used here.

into a microscopic mechanism of the decomposition and the recovery of this compound.

Decomposition and Recovery of Fe-Doped β″-Alumina

Here, we briefly describe general features of the decomposition and the recovery processes as investigated by means of X-ray powder pattern technique.

Specimens were obtained from those used for hot-pressing and annealing. Pellets of β″-alumina were prepared as described in earlier work (*6–8*). The composition of the pellet was $Na_2O \cdot 5.5\ (Al_{0.65}Fe_{0.35})_2O_{2.993}$. The ratio of the number of Fe^{2+} ions to the total number of Fe^{3+} ions, which was 0.021, was determined by a chemical analysis technique developed by Pastor earlier (*7*). For hot-pressing, the pellet was placed in a graphite die with a Li-doped β-alumina pellet used as a solid electrolyte, and, by applying a uniaxial pressure of 3000 psi, heated at 1150°C for 4 min under a constant flow of pure nitrogen gas. The annealing of the hot-pressed sample was made at 600°C for 5 days in air. X-Ray powder patterns

were taken from the original pellet, a, the hot-pressed sample, b, and the annealed sample, c, respectively, by utilizing Co$K\alpha$ radiation. The results are shown in Fig. 1.

The powder pattern of a is identified as that of a single phase β''-alumina. It has the rhombohedral symmetry and the observed lattice parameters based on the hexa-orthorhombic reference system are a_0 = 5.728 Å and c_0 = 34.26 Å. No other phases can be detected. On the other hand, the powder pattern of b shows that the specimen consists of three different phases; the β''-alumina phase, the spinel phase $Fe_{1+x}Al_{2-x}O_4$ and the β-Na-ferrite phase, $Na(Fe_yAl_{1-y})O_2$. Lattice parameters of the β''-alumina phase, however, are found to be smaller than those of the original phase by 1 to 2%; they are a_0 = 5.627 Å and c_0 = 32.82 Å. The lattice parameter of the spinel phase, which is cubic, is 8.147 Å, while those of the Na-ferrite, which has an orthorhombic structure, are a_0 = 5.38 Å, b_0 = 5.20 Å, and c_0 = 7.07 Å. The X-ray powder pattern for the annealed sample, shows that this is a single phase β''-alumina with the same lattice parameters as the original β''-alumina phase, a. Also a considerable broadening of the linewidths is observed here, indicating that the grain size of β''-alumina in c is far smaller than that in a. Because it is not possible to obtain the exact compositions of decomposition products nor the composition of the remaining β''-alumina phase in b, quantitative conclusions with respect to the decomposition reaction cannot be drawn only with these data.

Observation of the Decomposition and the Recovery by TEM

In order to obtain more detailed information with respect to the microscopic mechanism of decomposition and recovery processes, high resolution transmission electron microscopy was carried out on corresponding samples confirmed by X-ray powder diffraction. A JEM 200 CX electron microscope was used. Two types of specimens were prepared out of these samples for TEM observations. The one was made by ion-thinning, and the other was by crushing in an agate mortar and by mounting on carbon films. It is known that specimens are affected by preparations, and the results from these two types of specimens are compared carefully. Further, earlier studies of Mg-doped β''-alumina showed that decomposition was also caused by the irradiation of a strong electron beam during TEM observations (*9–11*). Therefore, in the present case, specimens were carefully observed with relatively weak electron beam, and no extensive radiation damages such as those reported earlier were detected. The microstructure observed in the starting β''-alumina, a, shows parallel array of stripes 11 Å apart which is the distance between conduction layers.

The observation of hot-pressed specimens prepared by ion-thinning method showed that the specimen consisted of grains with sizes around 10 μm, which was the same as the original phase. At grain boundaries and at junctions of three or four grains, a small amount of amorphous phases were observed. Since the amount of these amorphous phases was so small, they were not investigated further.

Each grain in b, however, is found to consist of three kinds of areas. Fig. 2a is a bright field image showing the existence of these areas. They are indicated by A, B, and C in the figure. Selected area diffraction shows that the area A is the remaining (undecomposed) β''-alumina and the area B, having a dark contrast, is the spinel phase. However, no diffraction pattern corresponding to Na-ferrite is obtained from areas C, which show a bright contrast and are distributed in the spinel phase. These areas give rise to halo patterns only, indicating that the structure is amorphous. De-

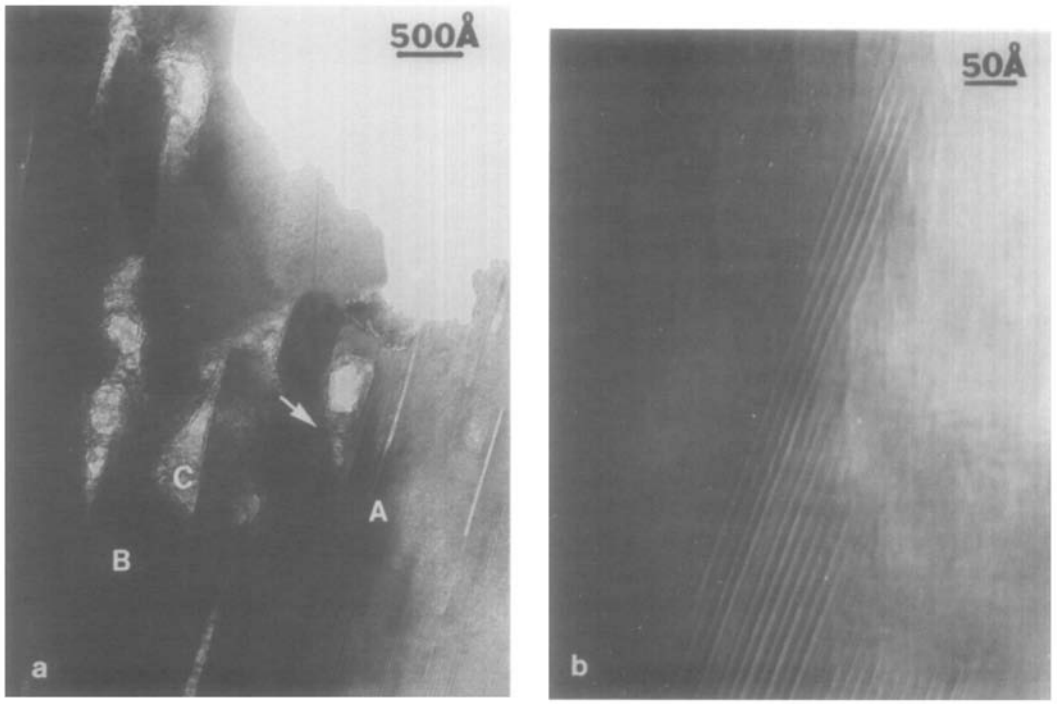

FIG. 2. (a) A bright field image of a decomposed specimen by hot-pressing. (b) A lattice image taken from an area indicated by an arrow in (a), showing the coexistence of β''-alumina and spinel.

spite careful observations, no area in the specimen shows the diffraction pattern corresponding to Na-ferrite. This suggests that areas C are originally Na-ferrite crystals but have changed into amorphous phase due to ion-thinning. Indeed, the amount of the amorphous substance coincides with that of Na-ferrite crystals which is estimated from the X-ray powder pattern. On the other hand, in crushed specimens, Na-ferrite crystals are found among β''-alumina and spinel crystals. Also, it is found that these Na-ferrite crystals gradually change into an amorphous phase due to irradiation of strong electron beam, giving rise to a similar diffraction pattern to that from the areas C. Therefore, it can be concluded that areas C are originally Na-ferrite crystals, but they have changed into an amorphous phase during the ion-thinning process.

The observation shows that the distribution of these three kinds of areas is not necessarily uniform over the entire specimen. In other words, some grains consist most of β''-alumina crystals with only a small amount of spinel and of amorphous phase. On the other hand, a few grains consist almost of spinel phase including islands of amorphous phase. Such a variation in microstructure from one grain to another means that the stage of decomposition varies from one area to another. Therefore, it is possible to find microstructures corresponding to various stages of decomposition from the observation carried out of a few number of specimens.

From the observation thus made, the following general conclusions with respect to the distribution of the three distinct phases can be drawn. (1) The β''-alumina phase always is of a single orientation in individual grains. This means that each grain is a sin-

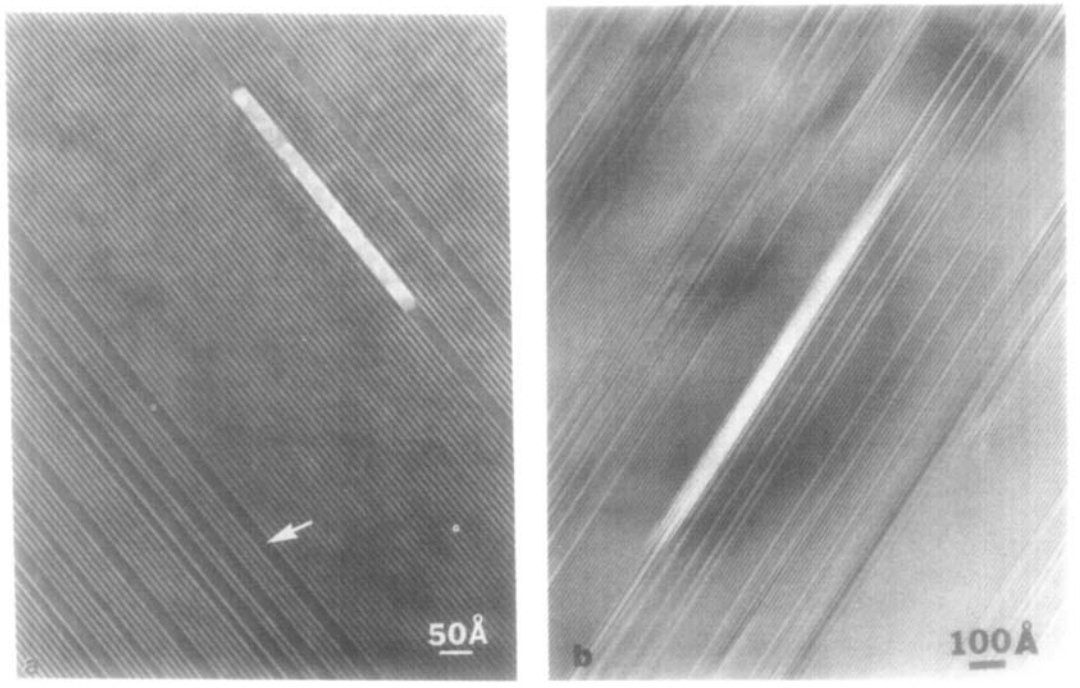

FIG. 3. High magnification images of the remaining β''-alumina phase.

gle crystal of β''-alumina before hot-pressing. (2) The amorphous phase is always distributed as islands among spinel crystals in a fashion shown in Fig. 2a. Sizes of these islands are at most 500 Å. (3) Spinel crystals are always coherently connected to β''-alumina crystals. An example of this coexistence is shown in Fig. 2b, which is a high magnification image of the boundary between a spinel and a β''-alumina crystal shown in Fig. 2a. The left side of the image is a spinel crystal while the right side is a β''-alumina crystal in which the conduction layers are seen as white parallel fringes with spacing of 11 Å. The image also shows that the (111) lattice fringes of spinel crystal, whose spacing is 4.8 Å, are exactly parallel to the conduction layers. This means that the oxygen sublattices of both crystals are common.

Figures 3a and b are images taken from a remaining (undecomposed) β''-alumina crystal. The incident electron beam is parallel to the (001) planes (the basal plane) in both cases. Therefore, the conduction layers can be seen as parallel white fringes in these images. They are periodically arranged with the spacing of 11 Å, indicating that these parts maintain the structure of β''-alumina. Between these regular arrangements of conduction layers, however, dark bands whose widths are larger than the normal spacing of conduction layers (white fringes) are observed. It is also seen that some dark bands are interrupted by small rectangular white islands. These bands are observed in decomposing β''-alumina crystals, although their widths, distribution density, and the sizes of white islands vary from one area to another. These features are also found in crushed specimens. On the other hand, these types of defects are not at all found in a. It is, therefore, concluded that these bands are found only at an

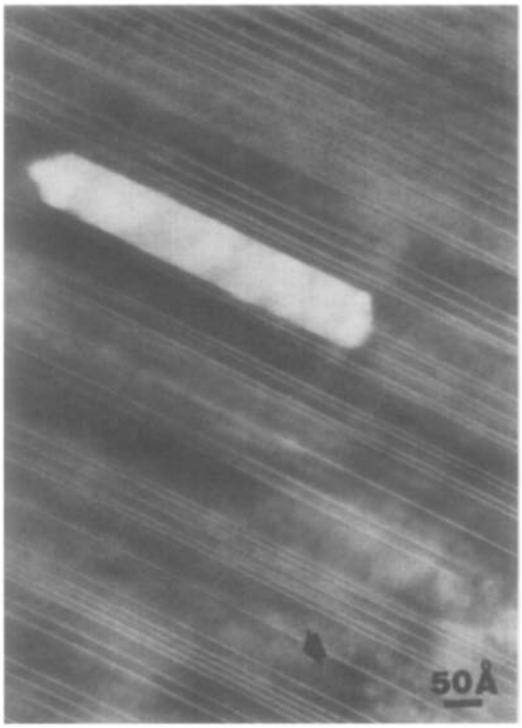

FIG. 4. A high magnification image of remaining β''-alumina near a boundary with a spinel crystal.

early stage of decomposition. Figure 4 is an image which is taken from an area close to the boundary of an undecomposed β''-alumina crystal and a spinel crystal. The beam direction is parallel to the [110] axis. The image shows that both the number and the width of dark bands and the size of a white island are much larger than those shown in Fig. 3. This shows that the size of these defects increases with the degree of decomposition.

Observations of undecomposed β''-alumina crystals with various beam orientations confirm that these plate-like defects are parallel to the (001) planes. Dark band defects are long, but some of them terminate within the crystals as seen in Fig. 3b. The width of these dark bands does not vary within one band, but it ranges from a few tens to a few hundreds Ångstroms. In particular, their width is always multiples of two S (spinel) blocks. For example, the width of a defect indicated by an arrow in Fig. 3a is 28 Å. This value is also the distance from one conduction layer (a thin white fringe in the image) to the third one in the c-direction of β''-alumina (11 Å × 3) minus the width of two conduction layers (2.5 Å × 2). The width of the thinnest defect created by the removal of one conduction layer, therefore, coincides with that of four S blocks or is equivalent to eight layers of close-packed oxygen layers. (The definition of the S block which is a unit building block of spinel and consists of two close-packed oxygen layers is given later; see Fig. 9.)

On the other hand, the width of white islands is not necessarily constant from one end to the other. As seen in Fig. 5, a white

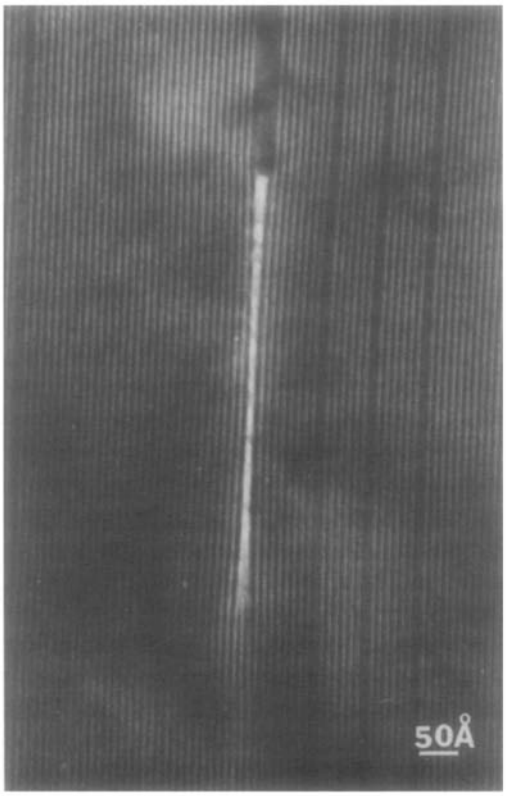

FIG. 5. A high magnification image showing an amorphous island in the remaining β''-alumina phase.

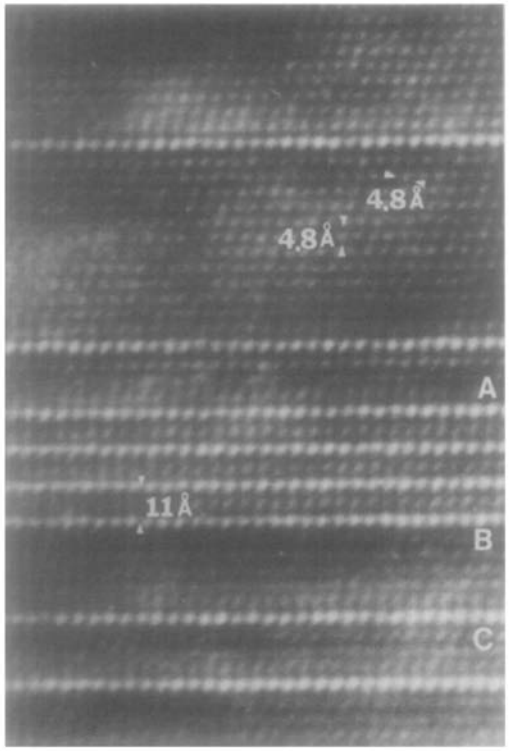

FIG. 6. The structure image of the remaining β''-alumina phase. The beam direction is in the [110] axis of the hexagonal lattice.

island becomes narrower toward its center, while the width at both ends is the same as that of a dark band connected to it. As a result, the surrounding β''-alumina crystal is heavily strained as seen from the bending of the image of the conduction layers. All islands observed have the same tendency. This indicates that white islands are foreign substance filling the space between two (001) plane of β''-alumina crystal. The degree of contraction at the center of islands, however, is not always the same. As seen in Fig. 5, the width of the island at the center is almost one-third less than that at the end, while others, as seen in Fig. 3a, have almost the uniform width. This variation is understood from the fact that the foreign substance takes the form of thin platelet and is contracted toward the center.

Now, let us discuss the fine structure of defects observed as dark bands. Figure 6 is a magnified image of the part indicated by an arrow in Fig. 4. In this figure, the area between A and B consisting of four lines of white dots is interpreted to be the β''-alumina structure. A line of white dots indicates a conduction layer and the distance between two lines is 11 Å as expected. In Fig. 7a, an image of the β''-alumina structure calculated under the corresponding condition to the micrograph is shown. The calculation was made based on the multislice method (*12*). In the calculation, a defocusing amount of −1200 Å, the thickness

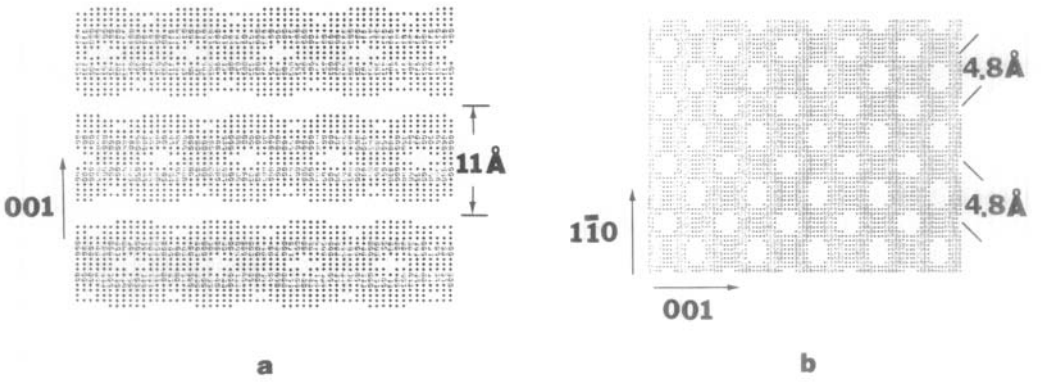

FIG. 7. Calculated images of (a) β''-alumina and (b) spinel ($FeAl_2O_4$). The beam direction is in the [110] of β''-alumina and in the [110] of the spinel.

of the crystal of 150 Å, and the spherical aberration coefficient of 2.8 mm were used as parameters. The defocusing amount was estimated from the width of the Fresnel fringe observed at the edge of the crystal. Effects of the beam divergence and chromatic aberration were also taken into account. In calculation, it is necessary to know the distribution of Fe and Al ions in the crystal. Since no data with respect to the distribution are available, the distribution in the spinel block is assumed to be the same as that in $FeAl_2O_4$ (*13*); Fe^{2+} ions occupy the tetrahedral sites while Al^{3+} ions occupy the octahedral sites. The calculated image satisfactorily reproduces the observed one between A and B as shown in Fig. 6.

The area between B and C is a part in which conduction layers of β''-alumina are removed. The image shows regular two dimensional fringes. The spacing of the fringes is 4.8 Å in both directions and the angle between them is about 70°. These values coincide with those of the {111} planes of the spinel structure viewed along the [110] direction. This indicates that the area has become a microcrystal of spinel with the close packed layers of oxygen ions parallel to those of the β''-alumina matrix. An image of the spinel structure with the [110] beam orientation calculated by using the same parameters as those for Fig. 7a is shown in Fig. 7b. Atomic parameters for $FeAl_2O_4$ (*13*) were used for this purpose. The agreement with the observed image shown in Fig. 6 is good. The fine structure between lines of white dots in other areas also are explained as the spinel structure. The coexistence of different phases in narrow bands with widths down to the size of unit cell is commonly called the microsyntaxy.

On the other hand, no crystalline image is observed from white islands. High resolution images of these islands are similar to those of the amorphous phase (area C in Fig. 2) found among spinel crystals. As pointed out earlier, these white islands are considered as precipitates of Na-ferrite which, however, have changed to an amorphous structure during ion-thinning.

TEM observations of annealed specimens show that most parts of the specimen are found to be the β''-alumina phase, but some parts consist of many microtwins with widths which range from a few tens to several hundreds Ångstroms. These twins are considered to be β''-alumina crystals formed during the recovery process. These newly formed β''-alumina crystals during the recovery process are not only faulty, but they are far smaller in their sizes, the original β''-alumina crystals being subdivided into several grains with different orientations of conduction layers. Small parts of spinel crystals, however, are yet occasionally found in areas among β''-alumina crystals. Figure 8 shows a high magnification image of one of these areas. In this figure, the right side (A) shows a β''-alumina crystal, and regular, ordered arrays of conduction layers are seen. The left side (B), is a defective spinel crystal. The incident beam was parallel to the [110] direction of the spinel crystal. As seen in the figure, the $(1\bar{1}1)$ planes of the spinel crystal are parallel to the conduction layers of the β''-alumina crystal. Therefore, the spinel crystal can be considered to be the decomposition product from the β''-alumina crystal seen in A. The area with the spinel structure (area B) shows parallel but irregularly spaced white fringes very similar to those of conduction layers in the β''-alumina crystal along the $(\bar{1}11)$ plane. These are the conduction layers created during the recovery process, and their spacings are yet irregular. This situation thus indicates the transitional stage of the recovery of spinel back into β''-alumina. However, they are not parallel to conduction layers of the original β''-alumina crystal at A (parallel to the $(\bar{1}11)$ plane). Since the spinel structure has four equivalent orientations of closed-packed oxygen

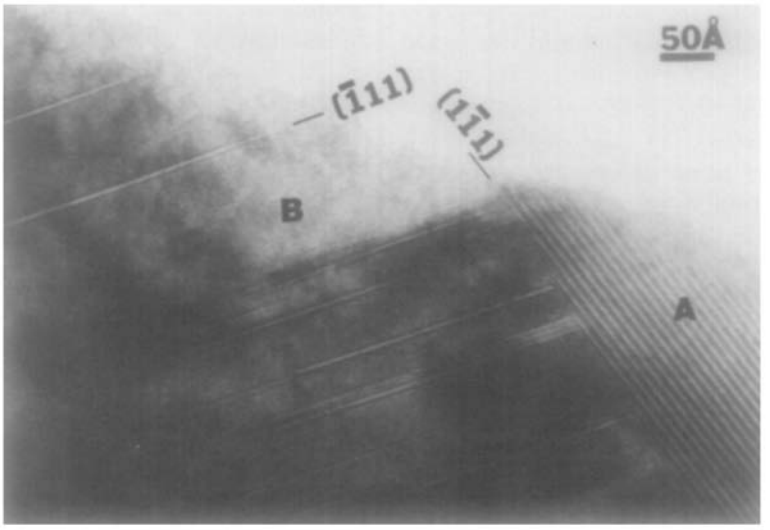

FIG. 8. A high magnification image of spinel in the annealed specimen. The beam direction is in the [110] direction.

layers, these newly formed conduction layers can take one of these four orientations. Some of the conduction layers in the spinel structure are connected with those in the β''-alumina structure.

Summary and Discussion

Results of X-ray powder diffraction (Fig. 1) show that a part of β''-alumina has decomposed into spinel and Na-ferrite, while the remaining (undecomposed) β''-alumina has changed its lattice parameters by hot-pressing at 1150°C in a reducing atmosphere. They also show a reverse reaction into β''-alumina which occurs upon annealing in air. By means of high resolution transmission electron microscopy of corresponding samples, various stages of reactions are identified. The results show how the decomposed phases are related to the original β''-alumina (Figs. 2–5) in their distributions, and how the interpretation of high resolution images of decomposed β''-alumina and spinel (Figs. 6–7) can be confirmed by image simulation. Figure 8 shows some processes by which the recovery of decomposed phases into β''-alumina occurs. The aim of this section is to synthesize all these data together to form a consistent picture with respect to the microscopic mechanism of the decomposition and the recovery.

The first step of the synthesis is to build up a reaction scheme of the decomposition and the recovery which satisfies the X-ray data. Since the exact composition of each phase of decomposed products is not obtained from the X-ray data only, reaction equations cannot uniquely be derived. Nevertheless, important conclusions regarding the reaction can still be obtained from the comparison of valence states of compounds involved in the reaction. In the starting β''-alumina, it was identified with a certain accuracy (~2%) that 98% of Fe ions are trivalent and the remaining Fe ions are divalent (*7*), while Na and Al ions should be in their normal valence states. In Na-ferrite, Na ions are monovalent, and all Fe and Al ions are trivalent. In spinel, on the other hand, one-third of metal ions is divalent, and these should be Fe ions, and the others in-

cluding Al ions are trivalent. If this is so, the amount of divalent Fe ions in spinel cannot be attributed solely to a small amount of Fe^{2+} ions which exist in the original β″-alumina. Therefore, it is concluded that a part of Fe^{3+} ions changes into divalent ions during the decomposition. In order to compensate for this change, some oxygen ions in β″-alumina should leave the specimen as oxygen gas molecules. The reaction formula then should take the form something like that shown by

$$Na_2O \cdot 5.5(Fe_{0.35}Al_{0.65})_2O_3 \rightarrow 2Na(Fe_{0.35}Al_{0.65})O_2 + 3(Fe_{0.35}Al_{0.65})_3O_4 + \tfrac{3}{2}O_2. \quad (1)$$

Here, it is also tentatively assumed that the ratio of Fe and Al ion in both spinel and Na-ferrite is the same as in the original β″-alumina. The equation indicates that one β″-alumina molecule decomposes to three spinel molecules, two Na-ferrite molecules, and 3/2 oxygen gas molecules. Equation (1) also indicates that the decomposition is basically a reduction process, agreeing with the fact that the hot-pressing is made under a constant flow of nitrogen gas. Indeed, heating a β″-alumina pellet in the same reducing atmosphere, but without applying pressure was also found to produce similar results in X-ray powder patterns, confirming the above conclusion.

Diffraction intensities of spinel and Na-ferrite were calculated based on Eq. (1) and compared with the observed diffraction pattern. The agreement was poor, indicating that some important factors were missing in Eq. (1). Although calculated intensity distributions for each compound agree well with observed ones, the amount of Na-ferrite with respect to that of spinel are considerably smaller than those expected from Eq. (1) as judged from their relative intensities. This indicates that not all Na ions of decomposed β″-alumina contribute to the formation of Na-ferrite. On the other hand, X-ray powder pattern shows that the lattice parameters of remaining (undecomposed) β″-alumina decrease substantially from those of the original phase. This indicates that undecomposed β″-alumina also participates in the reaction. An earlier study of Fe-doped β″-alumina shows that the lattice parameters decrease as the content of Na ions increases (*6*). For example, lattice parameters of $Na_2O \cdot 4(Al_{0.5}Fe_{0.5})_2O_3$ are 5.779 and 34.48 Å, respectively, while those of $Na_2O \cdot 7(Al_{0.5}Fe_{0.5})_2O_3$ are 5.784 and 34.67 Å, respectively. Therefore, the result indicates that a substantial part of Na ions of decomposed β″-alumina flows into the remaining (undecomposed) β″-alumina rather than forming Na-ferrite. The content of Na ions in the remaining β″-alumina can be estimated by extrapolating the lattice parameters of those obtained in the earlier study. They are located beyond the phase range of β″-alumina reported in the reference and this fact indicates that the remaining β″-alumina is supersaturated with Na ions. In order that the accommodation of extra Na ions be a part of the reaction, this fact should rather be interpreted that the content of Na ions in the remaining β″-alumina is that of the equilibrium value under the condition of hot-pressing.

The recovery reaction of the decomposed specimen can readily be understood from the above arguments. The decomposition is caused by a reducing atmosphere at high temperatures. Therefore, the decomposed phases can recover to the single phase of β″-alumina if they are heated in an oxidizing atmosphere.

Before discussing the results of high resolution TEM, it may be worthwhile to discuss briefly the structural relation between β- and β″-alumina and spinel. In discussing the β-alumina type compounds, one of the authors concluded that this type of compounds is built up of two structural unit blocks, D and S, and that the structure of a family of β-alumina type compounds is rep-

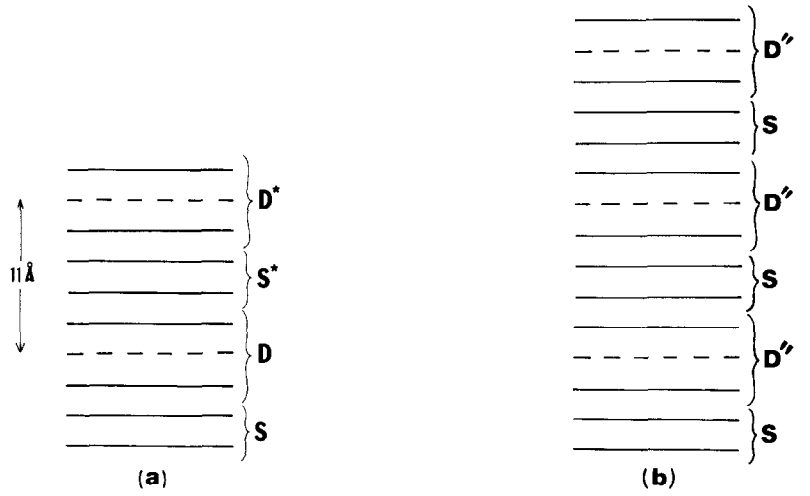

FIG. 9. Schematic representation of the structures of (a) β-alumina and (b) β''-alumina.

resented by the formula D(nS)D*(nS*)(n = 0, 1, 2, . . .) (*14–16*). Structural unit blocks D* and S* are the same as D and S but are rotated by 180° with respect to the c-axis and the value of n determines the period of a particular compound. The ordinary β-alumina corresponds to the structure n = 1. The definition of the D and the S block is given in reference to Fig. 9 of the n = 1 structure. Solid lines correspond to close-packed layers of oxygen ions and dotted lines indicate loose oxygen layers or the conduction layers. The S block consists of two close-packed oxygen layers and is the unit building block of spinel, while the D block includes the loose, conduction layer between two close-packed oxygen layers. Metal ions (except Na ions) exist between the close-packed layers and the tetrahedral sites exist only in the central block of the S. Although the whole part between two conduction layers is commonly called the spinel block, we limit the usage of the spinel block only to the S block because the D block does not have tetrahedral sites for metal ions. On the other hand, β''-alumina type compounds having the rhombohedral symmetry can then be described as [D″(nS)]$_3$ by utilizing the Zhudanov notation where D″ with the rhombohedral stacking symmetry corresponds to D of β-alumina. Again, the normal β''-alumina corresponds to the n = 1 compound. The structures of β- and β''-alumina are different only in the stacking of oxygen close-packed layers at both sides of the conduction layer. Although structurally the same, the S block in β-alumina type structures is not electrically neutral, the tetrahedral sites being occupied by trivalent ions.

Observations of the remaining (undecomposed) β''-alumina by high resolution electron microscopy show the formation of thin plate-like defects (dark bands) in the early stage of the decomposition. These defects are parallel to conduction layers and sometimes accompanied by small islands of amorphous phase (white islands) which is considered to have changed from Na-ferrite during the ion-thinning process. Along with the image simulation, these defects (dark bands) are confirmed to have the structure of spinel. It is also shown that the orientation of close-packed oxygen layers in these defects is exactly parallel to those of surrounding β''-alumina. By referring to Fig. 9,

these results suggest that the planar defects were formed by a conversion of the D″ blocks to the S blocks as a result of the collapse of conduction layers. The structure of the original S blocks is kept intact. That the defects have thickness which is an integral multiple of the thickness of two S blocks confirms this mechanism.

The mobility of Na ions in the conduction layer is extremely large. Therefore, the main microscopic process of the initial stage of the decomposition should be the transport of Na ions into the remaining β″-alumina. As stated earlier, X-ray diffraction results indicate that Na ions move out from decomposing β″-alumina into remaining β″-alumina. In other words, they show that remaining β″-alumina becomes supersaturated with Na and that the amount of Na-ferrite is far smaller than that expected from the reaction Eq. (1). Thus we conclude that the reaction starts as the flow of Na ions into remaining β″-alumina. The removal of a large amount of Na ions then results in the collapse of the conduction layers, and some oxygen ions possibly leave in the form of the oxygen molecule, with remaining Na ions and some metal ions along with some oxygen ions in the D″ blocks form precipitates of Na-ferrite, leading to the conversion of the D″ block into the S block as observed as the formation of spinel (Fig. 6).

Combining all observed evidences together, the microscopic mechanism of the decomposition in the reducing atmosphere such as the present case can be summarized as follows:

The reaction starts locally as the diffusion of Na ions in the conduction layers from decomposing β″-alumina into the surrounding β″-alumina in order to reestablish proper Na content in the surrounding β″-alumina under the reducing atmosphere at 1150°C. The loss of Na ions from the conduction layers results in the collapse of conduction layers of decomposing β″-alumina. As a result, some oxygen ions leave from the local decomposing β″-alumina as O_2 molecules, and the remaining oxygen ions along with remaining Na ions and some metal ions (Al^{3+} ions and Fe^{3+} ions in the D″ blocks) form precipitates of Na-ferrite. The amount of Na-ferrite is thus determined by the amount of remaining Na ions and is far smaller than that expected from Eq. (1). The loss of oxygen ions as oxygen molecules locally creates charge imbalance, but, in order to compensate for the imbalance, some Fe^{3+} ions in the decomposing β″-alumina should change into Fe^{2+} ions. The analysis of the content of Fe^{2+} and Fe^{3+} shows that the tetrahedral sites in the S block of β″-alumina are mostly occupied by trivalent ions. At the same time, by the redistribution of the remaining metal ions the D″ blocks transform into the S blocks, leading to the formation of spinel. The removal of oxygen ions from the decomposing β″-alumina, however, was not confirmed directly.

The microscopic mechanism of the recovery can be explained as the reverse reaction of the above. Upon heating in oxidizing atmosphere, the Na content in the remaining β″-alumina becomes supersaturated and the excess Na ions thus tend to flow out. At the same time, in the presence of Na, β″-alumina structure is more stable than spinel and Na-ferrite in the oxidizing atmosphere. Hence, the reconstruction of the D″ blocks occur along the {111} planes of spinel by the flow of Na ions from the remaining β″-alumina as well as from Na ferrite precipitates. Figure 8 shows this mechanism clearly. The creation of the D″ block from the S block is a growth of the conduction layers along the {111} plane in a microsyntactic fashion very similar to that of the creation of the CS planes in the Magnéli phase compounds such as V_nO_{2n-1} and Ti_nO_{2n-1} in VO_2 or TiO_2 with the rutile structure. This mechanism results in the subdivision of the original (decomposed)

β''-alumina and creates the broadening of X-ray lines.

Finally, it should be mentioned that there are some other important structural factors which enable these unique microscopic mechanisms of decomposition and recovery to occur. One is the weakness of bonding across the conduction layers of these compounds. The oxygen ions in the conduction layers do not form a close-packed arrangement unlike those in spinel blocks. Therefore, these oxygen ions can preferentially be removed from the crystal in a reducing atmosphere. Some earlier studies indicate that β''-alumina crystals are less stable than the normal β-alumina and this is attributed to the existence of extra bridging oxygen ions in the conduction layer of the latter (*17*). The addition of divalent dopants results in the removal of the bridging oxygen ions, and stabilizes the β''-alumina (*18*). The result of analysis of Fe^{2+} and Fe^{3+} ions, however, indicates that the tetrahedral sites of Fe-doped β''-alumina are occupied mostly by trivalent ions against this expectation. Another structural factor is the existence of Fe^{3+} ions. The change of these ions to Fe^{2+} ions can compensate excess charges due to the loss of oxygen ions from conduction layers or the increase of Na ions in them without destroying the structure of the spinel block. The existence of mixed valence Fe ions and, hence, the ease of redox reactions is essential in these unique decomposition and recovery mechanism explained above.

Acknowledgments

The present work was carried out under a partial support of NSF MRL program DMR 8020249 and NSF Grant DMR78-25236. Equipment provided through an NSF Grant DMR-78-09025 was crucial for the success of this work.

References

1. J. T. KUMMER, *Progr. Solid State Chem.* **7,** 141 (1972).
2. J. H. KENNEDY, *in* "Solid Electrolytes." (S. Geller, Ed.), p. 105, Springer-Verlag, Berlin (1977).
3. J. H. KENNEDY AND A. F. SAMMELLS, *J. Electrochem. Sco.* **119,** 1609 (1972).
4. C. A. BEEVERS AND M. A. S. ROSS, *Z. Kristallogr.* **96,** 59 (1937).
5. M. BELTMAN AND C. R. PETERS, *J. Phys. Chem.* **73,** 1774 (1969).
6. J. P. ROLAND, T. Y. TSENG, AND R. W. VEST, *J. Amer. Ceram. Soc.* **62,** 567 (1979).
7. R. G. PASTOR, Ph.D. thesis, Purdue University (1982).
8. T. Y. TSENG, Ph.D. thesis, Purdue University (1982).
9. L. C. DEJONGHE, *Mater. Res. Bull.* **12,** 667 (1977).
10. J. O. BOVIN, *Acta Crystallogr. Sect. A* **35,** 572 (1979).
11. Y. MATSUI AND S. HORIUCHI, *Acta Crystallogr. Sect. A* **37,** 51 (1981).
12. J. M. COWLEY, "Diffraction Physics," North-Holland, Amsterdam (1975).
13. I. GABALLAH, A. COUTOIS, F. JEANNOT, AND C. GLEITZER, *C.R. Acad. Sci. Paris* **280,** 1367 (1975).
14. H. SATO AND Y. HIROTSU, *Mater. Res. Bull.* **11,** 1307 (1976).
15. Y. HIROTSU AND H. SATO, *J. Solid State Chem.* **26,** 1 (1978).
16. H. SATO, H. KUWAMOTO, Y. HIROTSU, N. OTSUKA, AND G. L. LIEDL, *Rev. Chim. Miner.* **17,** 404 (1980).
17. W. L. ROTH, F. REIDINGER, AND S. J. LAPLACA, *in* "Superionic Conductors" (G. D. Mahan and W. L. Roth, Eds.), p. 223, Plenum, New York/London (1976).
18. D. R. WHITE, S. CHEN, H. R. HARRISON, AND H. SATO, *Solid State Ionics,* in press.